Nanoscale Cementite Precipitates and Comprehensive Strengthening Mechanism of Steel

JIE FU, GUANGQIANG LI, XINPING MAO, and KEMING FANG

This article summarizes the state of the art of the comprehensive strengthening mechanism of steel. By using chemical phase analysis, X-ray small-angle scattering (XSAS), room temperature organic (RTO) solution electrolysis and metal embedded sections micron-nano-meter characterization method, and high-resolution transmission electron microscopy (TEM) observation, the properties of nanoscale cementite precipitates in Ti microalloyed high-strength weathering steels produced by the thin slab continuous casting and rolling process were analyzed. Except nanoscale TiC, cementite precipitates with size less than 36 nm and high volume fraction were also found in Ti microalloyed high-strength weathering steels. The volume fraction of cementite with size less than 36 nm is 4.4 times as much as that of TiC of the same size. Cementite with high volume fraction has a stronger precipitation strengthening effect than that of nanoscale TiC, which cannot be ignored. The precipitation strengthening contributions of nanoscale precipitates of different types and sizes should be calculated, respectively, according to the mechanisms of shearing and dislocation bypass, and then be added with the contributions of solid solution strengthening and grain refinement strengthening. A formula for calculating the yield strength of low-carbon steel was proposed; the calculated yield strength considering the precipitation strengthening contributions of nanoscale precipitates and the comprehensive strengthening mechanism of steels matches the experimental results well. The calculated σ_s = 630 to 676 MPa, while the examined σ_s = 630 to 680 MPa. The reason that ''ultrafine grain strengthening can not be directly added with dislocation strengthening or precipitation strengthening'' and the influence of the phase transformation on steel strength were discussed. The applications for comprehensive strengthening theory were summarized, and several scientific questions for further study were pointed out.

DOI: 10.1007/s11661-011-0767-z

I. INTRODUCTION

STEEL is the fundamental material of a country's industrialization. Strength is one of the important performances of steel structures. For over half a century, ferrous-metallurgy and materials scientists from different countries have performed much in-depth research into steel's strengthening mechanisms. For single-phase alloy, Hall–Petch proposed the grain refinement strengthening theory[1,2] based on the dislocation pileup model. For steel in which second-phase precipitation exists, many authors proposed various kinds of precipitation strengthening mechanisms, based on the interaction between second-phase particles and dislocation motion, the most important of which are the shearing mechanism and bypass (looping) mechanism.[3–6]

JIE FU and KEMING FANG, Professors, are with the School of Metallurgical and Ecological Engineering, University of Science and Technology Beijing, Beijing 100083, P.R. China, and also with the Key Laboratory for Ferrous Metallurgy and Resources Utilization of Ministry of Education, China, Wuhan University of Science and Technology, Wuhan 430081, P.R. China. GUANGQIANG LI, Professor, is the Director of the Key Laboratory for Ferrous Metallurgy and Resources Utilization of Ministry of Education, China, Wuhan University of Science and Technology. Contact e-mail: ligq-wust@wust.edu.cn XINPING MAO, Chief Engineer, is with Guangzhou Zhujiang Steel Co., Ltd., Guangzhou 510730, P.R. China
Manuscript submitted March 29, 2010.
Article published online August 9, 2011

High-strength low-alloy (HSLA) steel containing microalloying elements such as V, Nb, and Ti is a typical steel with a precipitation strengthening mechanism, in which nanoscale V, Nb, and Ti carbides have a significant precipitation strengthening effect. However, because it is hard to determine the volume fractions of different types and sizes of nanoscale particles, by existing theoretical formulas, the contribution of precipitation strengthening to steel strength can only be analyzed in a qualitative way rather than by quantitative calculation, which prevents further research into steel's precipitation strengthening mechanisms.

Based on chemical phase analysis, X-ray small-angle scattering (XSAS), room temperature organic (RTO) analysis, high-resolution transmission electron microscopy (TEM), and steel tempering rapid-cooling technology, the precipitated nanoscale particles were quantitatively analyzed. The contribution of precipitation strengthening to the yield strength was calculated. Subsequently, the steel's strengthening mechanisms are discussed based on this calculation, and a comprehensive strengthening mechanism of steel is proposed.

II. NANOSCALE IRON-CARBON PRECIPITATES IN HSLC STEEL

Thin slab continuous casting and rolling process (referred to hereinafter as TSCR), one of the contem-

porary steel production processes, has been growing rapidly in the world in recent years. Over 95 pct of TSCR products are low-carbon steels with 0.06 to 0.25 pct carbon content or low-carbon high-strength alloyed steels. Higher strength is one of the significant mechanical properties of TSCR products. In studying the reasons for the high strength of TSCR's high-strength low-carbon (HSLC) steels, the authors of References 7 and 8 first found that there were a great number of nanoscale oxides and sulfides, whose sizes range from tens to hundreds of nanometers. They also found plenty of precipitation particles sized less than 20 nm, which have spinel-shape structure. The authors of References 9 and 10 found in their experiments that there existed nanoscale AlN particles in steel, whose size ranges from several to tens of nanometers, and they also did kinetic studies on these particles. The authors of References 11 and 12 studied the nanoscale carbides in TSCR's low-carbon steels and their influence on steel's mechanical properties and pointed out that there existed a great number of precipitates (Figure 1) sized less than 20 nm in TSCR's low-carbon slabs, rolled pieces, and final products. They are mainly iron-carbon precipitates and have a significant precipitation strengthening effect in steels.

The types, size distribution, and volume fractions of precipitates with size less than 20 nm in TSCR's low-carbon steels were systematically studied by the authors of Reference 13. The contribution of iron-carbon precipitates to steel's strength was discussed. They pointed out that the precipitates' strengthening contribution to the yield strength of HSLC equals that of grain refinement strengthening.

A. *Tempering Rapid-Cooling Experiment*[13]

According to the Fe-C binary phase diagram, at temperature A1, the equilibrium carbon content in ferrite is 0.022 pct; at room temperature, it is less than 0.008 pct. Below temperature A1, with the drop of temperature, part of the supersaturated carbon will precipitate from ferrite. In the course of thin slab continuous casting and rolling, the great intensity of laminar cooling results in rapid cooling of the strips, the precipitates' size is small, their strengthening effects are great, and therefore, the TSCR steels have higher strengths. In coiling, on the other hand, the cooling rate of coils is slow, the precipitates are coarsened, and therefore, the steel's strength will be expected to be a bit lower than before the coiling.

Three special experiments were designed to study the precipitating temperature, precipitation, growth, coarsening, and strengthening effects of iron-carbon precipitates with size less than 20 nm. The first set of experiments studied the influence of treating temperature below A1 on the mechanical properties of steels (one more experiment was done to test the reproducibility of the results). The second studied the influence of treating time on steel's strength, and the experimented material was HSLC steel ZJ330 (coil no. 53921); the results are shown in Table I (the mechanical property of repeated experiments is represented by Tests 1 and 2)

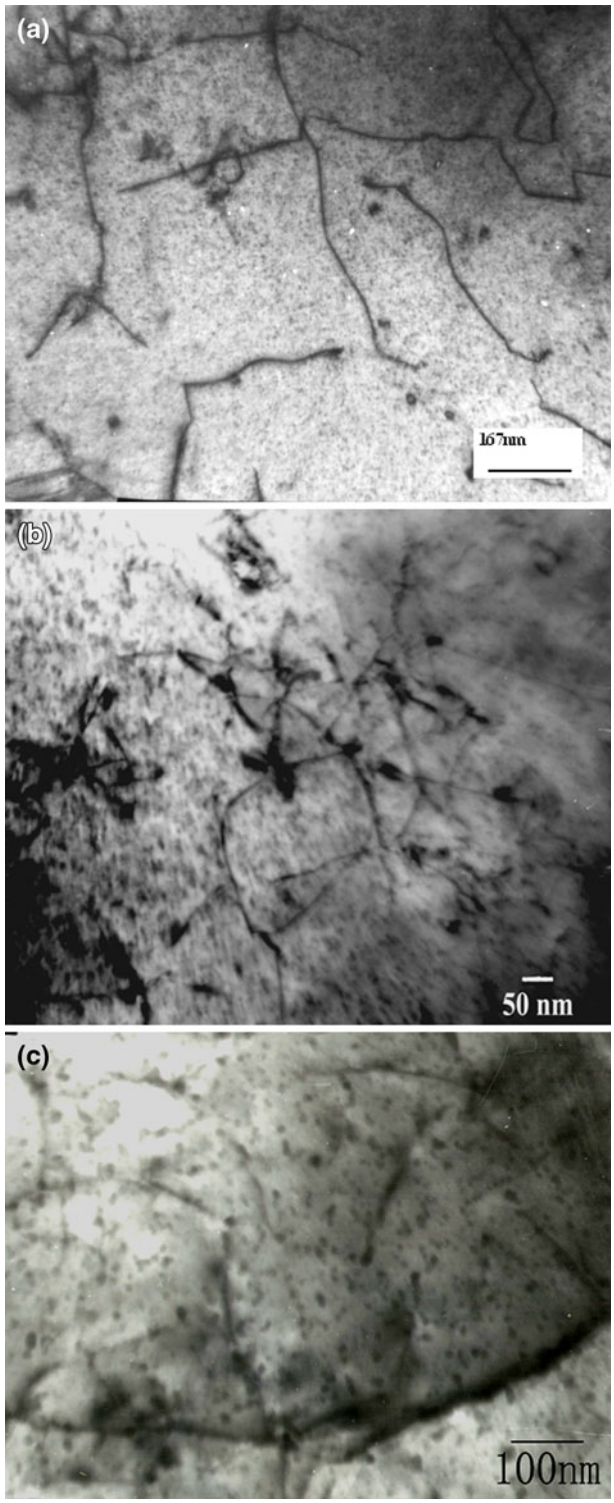

Fig. 1—TEM micrograph of nanoscale precipitates in HSLC: (*a*) slab, (*b*) rolled piece, and (*c*) product.[13]

and Figure 2. The third is the repeated experiment of the second, in which the experimented material is another coil of ZJ330 (coil no. 53931), and the σ_s, σ_b, and δ were 351 MPa, 425 MPa, and 42 pct, respectively; the results are shown in Figure 3.

From Table I and Figures 2 and 3, we can see that the cooling speed has a great influence on steel strength.

Table I. Effect of Tempering Temperature (Holding 20 Minutes) and Cooling Method on the Mechanical Properties of ZJ330 Steel

Number	Tempering Temperature [K (°C)]	Cooling Method	Yield Strength (MPa)		Tensile Strength (MPa)		Elongation (Pct)	
			Test 1	Test 2	Test 1	Test 2	Test 1	Test 2
1	original specimen		339	344	397	408	45	39
2	473 (200)	water	341	336	399	406	48	44
3	573 (300)	water	330	339	405	414	45	46
4	673 (400)	water	335	330	410	407	40	43
5	773 (500)	water	351	342	413	420	43	41
6-1	873 (600)	water	403	410	480	490	30	29
6-2	873 (600)	air	329	345	403	405	41	41
6-3	873 (600)	furnace cooling	320	322	397	397	43	43
7	973 (700)	water	468	458	651	625	13	16

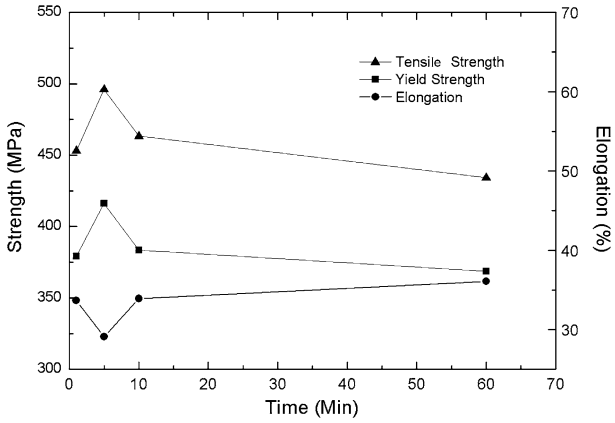

Fig. 2—Influence of tempering time on the mechanical properties of HSLC steel at the same temperature below A1.

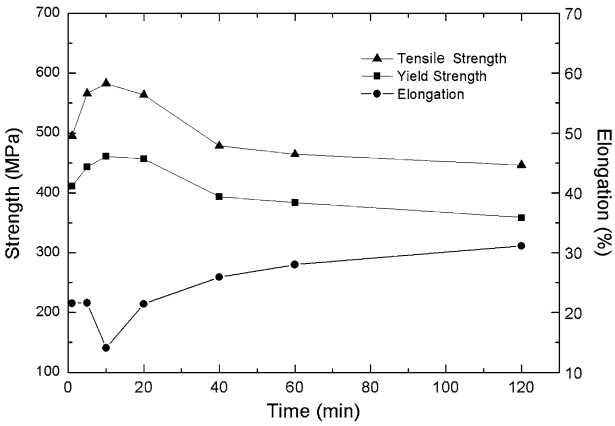

Fig. 3—Relation between tempering time of ZJ330 (coil no. 53931) steel and its performance.

When the temperature is above 873 K (600 °C) but lower than A1, tempering and fast cooling could increase steel strength significantly. As cooling speeds of steel during casting, rolling, and after coiling are all relatively fast in the TSCR process, a large amount of nanoscale participants include the size less than 20 nm participants that exist in slab, rolling pieces (steel sheets stuck in rolling processes), and products (finished plates); the experimental results match the expected results mentioned previously, indirectly proving the existence of nanoscale iron carbide precipitates, as shown in Figure 1.

B. *Analysis Using High-Resolution TEM*

Liu *et al.*[8] found a large number of 50- to 60-nm Fe-O-C participants near ferrite grain boundaries in HSLC steel. It is a bit difficult to observe particles with size less than 20 nm using an analytical electron microscope, particularly those with size only several nanometers, as it is quite hard to determine whether these particles are iron-carbon precipitates because of the matrix effect disturbances. To determine the characters and precipitation mechanism of these particles, further observation of the precipitate particles extracted by the electrolysis method was done with high-resolution TEM.

During the experiments, the hot-rolled strip piece (3-mm thickness) was electrolyzed with organic solution for 24 hours, and then the particles obtained from electrolysis were put into dehydrated alcohol solution. After ultrasonic vibrating, the fine particles floating on the upper layer were sucked with a chemical dropper and dipped onto a copper microgrid; finally, the sample for TEM was obtained when all the dehydrated alcohol was evaporated. The sample was observed with a high-resolution transmission electron microscope JEM2010 (JEOL Limited, Tokyo, Japan), with 500,000 times magnification and 200 kV voltage. The chemical composition of the powder was also analyzed with an X-ray energy spectrum. The results are shown in Figure 4.

From Figure 4, it can be seen that there are a large number of Fe-O-C precipitates with sizes less than 10 nm. Figure 4(b) is the energy spectrum of the center particle (about 10 nm) of Figure 4(a).

C. *Chemical Phase Analysis and XSAS*

It is quite difficult to determine the mass fraction or volume fraction of nanoscale particles in steel with an electron microscope, yet the volume fractions of precipitates with different sizes are indispensable for calculating the strength of steel. Chemical phase analysis and XSAS are effective methods to determine the chemical

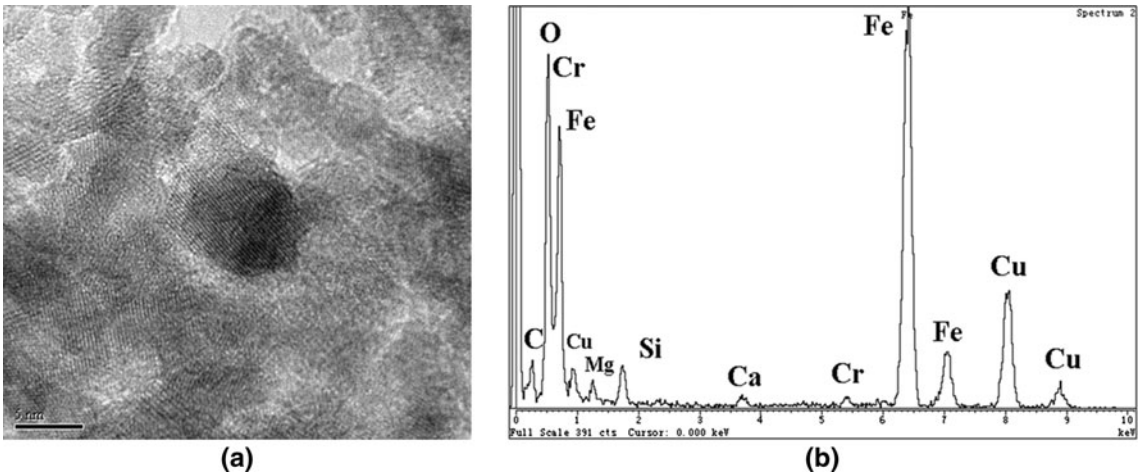

Fig. 4—(*a*) High-resolution TEM image of electrolytic nano Fe-O-C precipitate and (*b*) EDS from ZJ330 steel.

Table II. Chemical Composition (Mass Percent) of Testing Steels*

Testing Materials	C	Si	Mn	S	P	Cu	Total Al	Acid Solvable Al	N	Total O
ZJ330 hot-rolled plates	0.060	0.11	0.28	0.006	0.012	0.12	0.020	0.016	0.0044	0.0028
ZJ330 slab	0.051	0.04	0.39	0.012	0.015	0.16	0.031	0.0306	0.0044	0.0030
ZJ330 rolling piece	0.051	0.04	0.39	0.012	0.015	0.16	0.031	0.0306	0.0044	0.0030
ZJ510 hot-rolled plates	0.18	0.28	1.21	0.004	0.023	0.11	0.024	0.021	0.0034	0.0024

*The analysis results of tramp and impurity elements in ZJ330 and ZJ510 steel in EAF-CSP process:Ni 0.061 pct, Cr 0.034 pct, Mo 0.011 pct, V 0.010 pct, Nb 0.004 pct, Ti 0.014 pct.

Table III. Size Distribution of Cementite Particles with Size Less than 18 nm Precipitated in ZJ330 and ZJ 510 Steels

Tested Materials	Total M_3C in Steel, Mass Pct	Ratio of Various Sizes of Particles*				<18-nm Particles, Mass Pct
		1 to 5 nm	5 to 10 nm	10 to 18 nm	<18 nm	
ZJ300 hot-rolled plates	0.888	0.25/1.0	0.53/2.7	0.28/2.2	—/5.9	0.052
ZJ330 slab	0.749	0.30/1.2	0.65/3.7	0.47/3.7	—/8.2	0.061
ZJ330 1st pass rolling piece	0.755	0.47/1.9	0.99/4.9	0.82/6.6	—/13.4	0.101
ZJ510 hot-rolled plates	2.278	0.21/0.8	0.46/2.3	0.11/0.9	—/4.0	0.091

*Numerator—$f(D)$, average M_3C mass percentage in 1-nm range, pct/nm; and denominator—the total M_3C mass percentage in different size ranges in steel.

composition, mass fraction, or volume fraction of nanoscale particles with different sizes.

Chemical phase analysis can be described as the following processes:

(1) electrolyzing the steel sample to obtain electrolyzed powders containing iron carbonitride $Fe_3(C_xN_y)$, alloy carbonitride M (C_xN_y), sulfides, and nitrides;
(2) getting rid of iron carbide, sulfides, and AlN to obtain M (C_xN_y) and oxides; and
(3) removing M (C_xN_y) phase to get stable oxides.

After the preceding separation procedures, the electrolyzed powders were dissolved, respectively; the contents of Fe, Mn, Ni, N, and carbon were analyzed; and then the mass fraction of cementite based on the molecular formula $(Fe_aMn_bNi_c)_3(C_xN_y)$ was calculated.

According to GB/T 1322191 (ISO/TS 13762 2001), the particle size distribution of precipitate powders was analyzed by SAXS with a Kratky small-angle scattering instrument (Rigaku Corporation, Tokyo, Japan) of X-ray diffraction spectroscopy; the analyzed error is less than 10 pct. The chemical compositions of experimental steel and results are shown in Tables II and III, respectively.

The thickness of the EAF-CSP ZJ330 slab is 50 mm, and it reduced to 25 mm after the first rolling pass. The start rolling temperature is 1363 K (1090 °C), the exit temperature is 1325 K (1052 °C) for the first pass rolling, the finishing rolling temperature is 1163 K (890 °C), and the coiling temperature is 913 K (640 °C).

III. NANOSCALE IRONCARBON PRECIPITATES IN HSLA STEEL

HSLA steel refers to the steel containing microalloying elements such as V, Nb, and Ti. The Ti microalloyed high-strength weathering steel is an HSLA steel.

Chemical phase analysis and XSAS analysis were carried out on the samples of HSLA steels and Ti microalloyed high-strength weathering steel. The mass fractions of M_3C and MC particles less than 36 nm in the electrolytic powders were measured. The chemical compositions of experimental steel and results of HSLA steel are shown in Tables IV and V, respectively.

From Tables IV and V, it can be seen that the mass fraction of $M(C_xN_y)$ in the particles with size less than 36 nm is much less than that of $M_3(C_xN_y)$ with the same size in steel.

The Ti microalloyed high-strength weathering steel under lab[14] and production conditions[15] was studied, and it was found that Ti microalloying has an obvious influence on the strength of hot-rolled strips. The authors of Reference 15 studied the strengthening mechanism of Ti using chemical phase analysis, XSAS, and electron microscope analysis, and they found that the percentage content of nanoscale TiC increases with the increase of Ti content in steel; as a result, the steel's yield strength increases. They concluded that Ti strengthening mainly comes from TiC's precipitation strengthening. The calculated results do not match the actual measured strength, as the influence of Fe_3C precipitates was not considered. This article studied the size distribution and mass percentage of Fe_3C and TiC in Ti microalloyed steels produced by TSCR process.

Tables VI through X show the precipitates' structural parameters, mass fraction of elements in M_3C and MC in steel, size distribution of M_3C and MC precipitates in the no. 2 sample of Table IV, and mechanical properties of experimental steel, respectively.

Table VI shows the structural parameters of precipitates obtained by X-ray diffraction for the extracted particles by electrolysis. Table VII shows the mass fraction of precipitated phases in steel; from Table VII, it can be seen that the biggest mass fraction of the precipitated phase is M_3C cementite-based compounds, followed by Ti (C, N); the mass fraction of M (C, N) equals that of steel containing 0.09 pct Ti in Reference 15. The size distributions of Fe_3C and MC precipitates in the no. 2 sample of Table IV determined by XSAS are shown in Tables VIII and IX, respectively.

To further study the existence of nanoscale iron carbon precipitates in HSLA steels, the RTO metal embedded sections micron-nanometer characterization method[16] was used to prepare the sample, and it was analyzed with high-resolution TEM.

The RTO metal embedded sections micron-nanometer characterization method (hereinafter referred to as

Table IV. Chemical Compositions of Experimental Steel* (Mass Percent)

No.	C	Si	Mn	S	P	Al	N	Cu	Ni	Cr	Mo	V	Nb	Ti
70A	0.053	0.08	1.90	0.001	0.0060	0.029	0.0056	0.10	0.054	0.043	0.016	0.010	0.0600	0.125
B_2C	0.062	0.47	2.34	0.011	0.0038	0.210	0.0063	0.11	0.046	—	—	0.032	0.0044	0.029
No.1	0.061	0.10	2.10	0.010	0.0840	0.010	0.0009	0.03	0.030	0.060	—	—	—	0.085
No.2	0.059	0.40	0.41	0.002	0.0740	0.030	0.0070	0.25	0.180	0.410	—	—	—	0.090

*70A, B_2C, and No. 1 steels were laboratory tested steel sheets, with 6-mm thickness; and No. 2 steel was the product of industry process, with 3-mm thickness.

Table V. Size Distribution of Carbide Particles with Size Less than 36 nm Precipitated in 70A and B_2C Steel (Mass Percent)

Grade	Particle Types	Amount of Particles in Steel (Mass Pct)	Percentage of Various Size of Particles in Specimen*				Particles Less than 18 nm in Steel (Mass Pct)	Particles Less than 36 nm in Steel (Mass Pct)
			1 to 5 nm	5 to 10 nm	10 to 18 nm	18 to 36 nm		
70A	$M_3(C_xN_y)$	0.3109	0.77/3.1	1.59/8.0	0.68/5.4	0.93/16.8	0.0513	0.1035
	$M(C_xN_y)$	0.0895	1.05/4.2	2.15/10.7	1.26/10.1	0.91/16.4	0.0224	0.0371
B_2C	$M_3(C_xN_y)$	0.4865	0.06/0.2	0.19/1.0	0.23/1.8	1.46/26.3	0.0146	0.1425
	$M(C_xN_y)$	0.0575	0.30/1.2	0.65/2.2	0.23/1.8	0.47/8.4	0.0036	0.0084

*Numerator—$f(D)$, average $M_3(C_XN_Y)$, or $M(C_XN_Y)$ mass percentage in 1-nm range, pct/nm; and denominator—the total $M_3(C_XN_Y)$ or $M(C_XN_Y)$ mass percentage in different size ranges in steel.

Table VI. Structural Parameters of Precipitate

Phase	Lattice Constant, nm	Crystal Structure	Structural Formula
M_3C	a_0 = 0.45 to 0.45 b_0 = 0.51 to 0.51 c_0 = 0.67 to 0.67	orthorhombic	$(Fe_{0.955}Cr_{0.035}Mn_{0.010})_3C$
Ti(C, N)	a_0 = 0.42 to 0.42	face-centered-cubic	$(Mo_{0.022}Nb_{0.006}Ti_{0.972})(C_{0.661}N_{0.339})$
TiC	a_0 = 0.43 to 0.43		
Ti_2CS	a_0 = 0.32, c_0 = 1.12 c/a = 3.5	hexagonal	

Table VII. Mass Fraction of Elements in M_3C and MC in Steel, Mass Percent

Phase	Mass Fraction in Steel of Elements					Mass Fraction of Phase in Steel
Fe_3C	Fe	Cr	Mn	C		
	0.4937	0.0167	0.0051	0.0371		0.5526
M(C, N)	Mo	Nb	Ti	N	C	
	0.0037	0.0010	0.0814	0.0083	0.0139	0.1083
AlN	Al	N				
	0.0015	0.0008				0.0023
Ti_2CS	Ti	C	S			
	0.0102	0.0013	0.0034			0.0149

Table VIII. Size Distribution of M_3C Precipitates in Number 2 Sample of Table IV

Size Range (nm)	$f(D)$ (Pct/nm)	Mass Fraction in Total M_3C Particles (Pct)	Accumulated Mass Fraction (Pct)
1 to 5	3.39	13.5	13.5
5 to 10	2.13	10.7	24.2
10 to 18	2.34	18.7	43.0
18 to 36	0.49	8.8	51.8
36 to 60	0.28	6.8	58.6
60 to 96	0.31	11.1	69.7
96 to 140	0.24	10.5	80.2
140 to 200	0.16	9.8	90.0
200 to 300	0.10	10.0	100.0

Table IX. Size Distribution of MC Precipitates in Number 2 Sample of Table IV

Size Range (nm)	$f(D)$ (Pct/nm)	Mass Fraction in Total MC Particles (Pct)	Accumulated Mass Fraction (Pct)
1 to 5	2.13	8.5	8.5
5 to 10	1.75	8.8	17.3
10 to 18	1.49	12.0	29.3
18 to 36	0.49	8.7	38.0
36 to 60	0.31	7.3	45.3
60 to 96	0.22	8.1	53.4
96 to 140	0.23	10.1	63.5
140 to 200	0.19	11.3	74.7
200 to 300	0.25	25.3	100.0

In sample no. 2, the average size of M_3C precipitates is smaller than that of MC precipitates.

the RTO characterization method) is a method to embed the micron-nanometer section sample with metal in the organic solution at room temperature. This method solves the problem of cutting nanoscale films from bulk materials such as steel to observe micron-nanoscale particles; it has been widely used in the research of micron-nanoscale materials.[16,17] The steps of cutting nanoscale films from micron-nanoscale materials were described in References 16 and 17.

Using the RTO method, the experimental hot-rolled steel strip piece was electrolyzed in an organic solution for 24 hours, and dehydrated alcohol was used to disperse the electrolyte containing nanoscale precipitates onto the copper foil; then, the nanoscale precipitates on copper foil were embedded by electroplating copper with the aforementioned RTO method. Then, the sample thickness was reduced by means of polishing and an ion thinning instrument to the extent where an electron beam can get through the sample; following this, the sample was observed with high-resolution TEM.

Figure 5 is a TEM morphology picture of a RTO sample made from the precipitates extracted by electrolysis from the experimental steel. From this picture, it can be seen that more precipitates are of size less than 20 nm and are of polygonal shape rather than circular and oval.

Figures 6 and 7 are the typical energy spectra of Fe_3C and TiC precipitates, respectively, in RTO samples, from which the element's atom percentage can be roughly judged. It is hard to accurately identify the phase composition of precipitates according to EDS results, because the sizes of the nano precipitates are very small.

Figures 8 through 10 are high-resolution images and the electron diffraction pattern of Fe_3C and M(C, N) precipitate, respectively, in RTO samples prepared from steel no. 2 in Table IV.

IV. CONTRIBUTION OF NANOSCALE IRON-CARBON PRECIPITATES TO STEEL'S PRECIPITATION STRENGTHENING

A. *Theoretical Formula of Precipitation Strengthening*

Precipitation strengthening is a strengthening method in which the interaction between dispersed fine precipitation phases and the dislocations in steel obstructs the movement of dislocations, thus increasing the strength of steel.

Two types of interactions occur when the moving of dislocations is obstructed by the precipitation phase; as a result, two types of strengthening mechanisms occur. One is called the shearing (cutting) mechanism where dislocations cut the particles; the other is called the bypass (looping) or Orowan mechanism where the dislocations do not penetrate the particles, but bypass them, forming a dislocation loop around the particles.

The precipitation strengthening effect of fine precipitates in steel can be calculated through the simplified formula [1] proposed by Gladman *et al.*[3] based on

Table X. Mechanical Properties of Experimental Steels*

No.	Thickness (mm)	Ti Content (Pct)	$\sigma_{0.2s}$ (MPa)	σ_b (MPa)	δ (Pct)	$\sigma_{0.2s}/\sigma_b$
1	6	0.085	648	749	16.4	0.9
2	3	0.090	630 to 680	680 to 730	21	0.88

*$\sigma_{0.2s}$, nominal yield strength R_{eL}; and σ_b, tensile strength R_m.

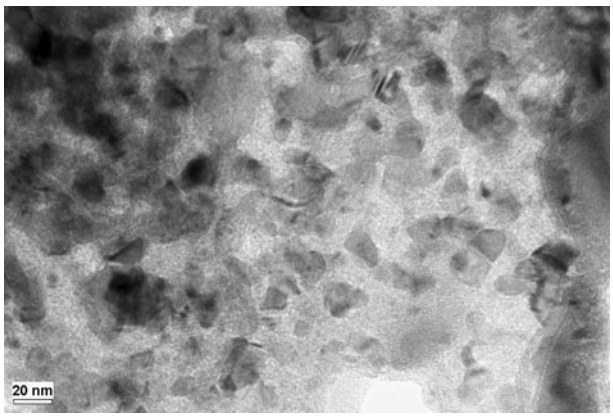

Fig. 5—TEM photograph of RTO sample for precipitates extracted from experimental steel no. 2 in Table IV.

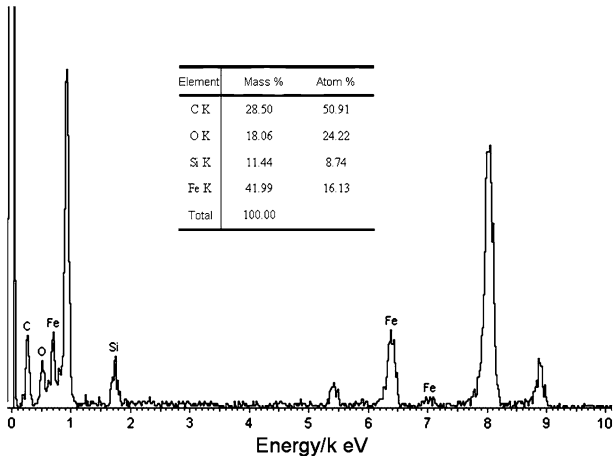

Fig. 6—XEDS spectrum of Fe_3C precipitate in RTO sample prepared from steel no. 2 in Table IV.

Ashby–Orowan's revised model. When the average diameter of particles is greater than 40 nm, the contribution of precipitation strengthening is not that much.

$$\sigma = \frac{5.9\sqrt{f}}{\bar{x}} \times \ln\left(\frac{\bar{x}}{2.5 \times 10^{-4}}\right) \quad [1]$$

where σ = the precipitation strengthening contribution to the yield strength (increment), MPa; $\bar{x}$ = the diameter of precipitates plane intercept, μm; and f = the volume fraction of precipitation phase.

When the diameters of precipitates are very small, and the interface tension between them and the matrix is small, the precipitation is coherent or semicoherent, from[4]

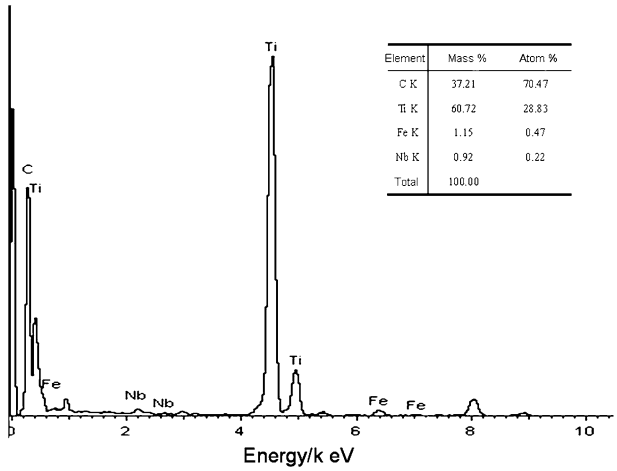

Fig. 7—XEDS spectrum of TiC precipitate in RTO sample prepared from steel no. 2 in Table IV.

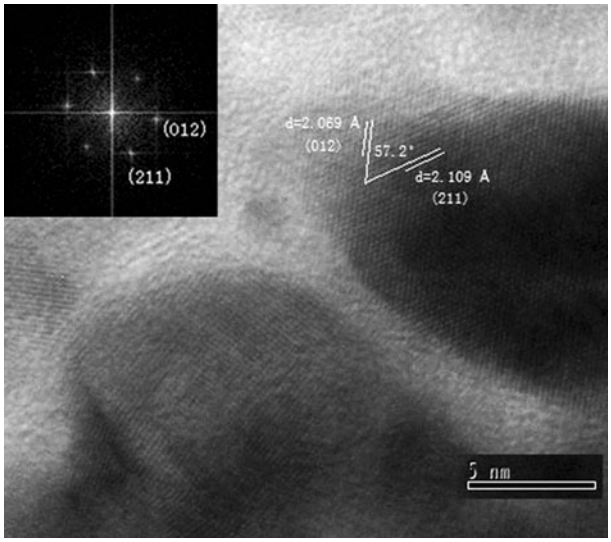

Fig. 8—High-resolution image of Fe_3C precipitates in RTO sample of Ti microalloyed high-strength weathering steel (no. 2 in Table IV).

$$\sigma = \overline{M}\tau_P = \frac{2 \times 1.1}{\sqrt{2AG}} \times \frac{\gamma^{3/2}}{b^2} \times d^{1/2} f^{1/2} \quad [2]$$

where τ_p = the shear stress caused by the dislocations cutting with particles, MPa; $A = \frac{1}{2\pi K}\ln\left(\frac{d}{2b}\right)$ = the dislocation line tension function; $K = (1 - \nu)$ for edge type dislocation, $K = 1$ for screw dislocation, and

$\frac{1}{K} = \frac{1}{2}\left(1 + \frac{1}{1-v}\right)$ for mixed type dislocation; v = Poisson's ratio $v = 0.291$; b = the absolute value of the dislocation's Burgess vector, $\mathbf{b} = 0.248$ nm; G = the shear elasticity modulus, 80,650 MPa; γ = interface energy between precipitates and the matrix, $\gamma = 0.5$ to 1 J/m^2; d = the second-phase particle diameter, μm; f = the volume percentage; and $\overline{M}$ = the average Schmid orientation factor, $\overline{M} = 2$ for bcc iron.

From formulas [1] and [2], it can be seen that, when steel's second-phase precipitate strengthening is shearing (cutting) type, its strengthening effect is proportional to the half power of second-phase volume fraction and the half power of particle size d. When it is a bypass mechanism, its strengthening effect is proportional to the half power of the volume fraction and roughly inversely proportional to particle size d; that is, the strengthening effect of the shearing (cutting) mechanism increases with the increasing particle size, while the strengthening effect of the bypass mechanism deceases with the increase of particle size. The critical transformation size d_c can be calculated by the numerical solution of Eq. [3]:[5,6]

$$d_c = 0.209 \frac{Gb^2}{K\gamma} \ln\left(\frac{d_c}{2b}\right) \qquad [3]$$

The meanings of symbols in formula [3] are the same as mentioned previously. The critical transformation size of the precipitate depends on the properties of dispersed particles; the smaller the sizes and the smaller the interface energy between the precipitates and the matrix, the larger the d_c. Different types of precipitates have different d_c values.

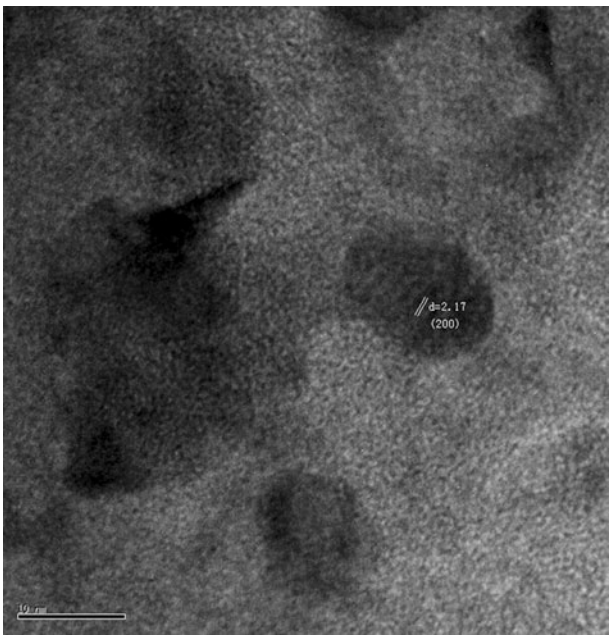

Fig. 9—High-resolution image of TiC precipitates in RTO sample of Ti microalloyed high-strength weathering steel (no. 2 in Table IV).

B. *Contribution of Nanoscale Iron Carbon Precipitates to Yield Strength in HSLC Steel*

Based on the size distribution, average diameters, crystal parameters, and mass fraction of different types of nano precipitants obtained, assuming the nanoscale precipitates have the same density with large size particles, the precipitation strengthening contribution could be quantitatively calculated.

According to formulas [1] through [3], and the data in Table III, the influence of nanoscale Fe_3C to the yield strength of HSLC steel's was calculated; the results are shown in Table XI.

From Table XI, it can be seen that, for ZJ330 with 0.06 pct carbon content, the contribution of precipitation strengthening increases with the increase of cooling speed of steel (the rolled piece is thinner than slab and its cooling is faster; though the final product is much

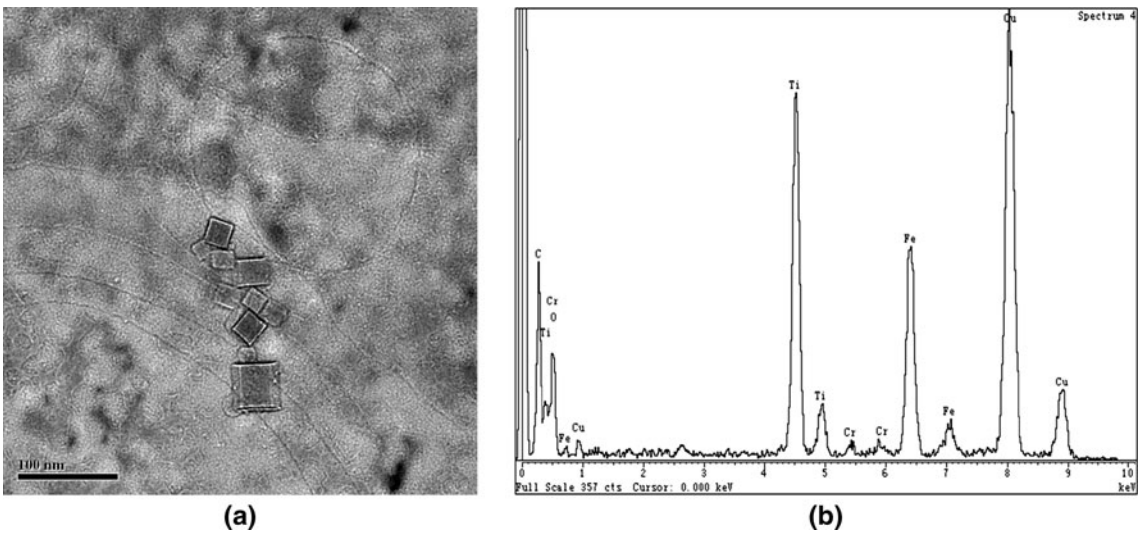

Fig. 10—(*a*) String of particles containing Fe, Ti, O, and C in ZJ510 microgrid sample and (*b*) its energy spectrum.

Table XI. Contribution of Fe_3C Precipitates Smaller than 20 nm to the Yield Strength of HSLC Steel (MPa)

Diameter Range, nm	ZJ330 Hot-Rolled Strip		ZJ330 Slab		ZJ330 Rolled Piece		ZJ510 Hot-Rolled Strip	
	Volume Fraction Pct	Yield Strength Increment	Volume Fraction Pct	Yield Strength Increment	Volume Fraction Pct	Yield Strength Increment	Volume Fraction Pct	Yield Strength Increment
1 to 5	0.00900	37.9	0.00912	38.2	0.01463	48.3	0.01859	54.5
6 to 10	0.02430	83.3	0.02810	89.6	0.03770	103.7	0.05339	123.5
11 to 18	0.01980	23.9	0.02810	28.4	0.05077	38.2	0.02091	24.5
Total	0.05310	145.1	0.06532	156.2	0.10309	190.3	0.09289	202.5

Table XII. Contribution of Fe_3C and Ti(CN) to the Yield Strength of Ti Microalloyed High-Strength Weathering Steel

Diameter Range, nm	Fe_3C		Ti(C,N)	
	Volume Fraction (Pct)	Yield Strength Increment (MPa)	Volume Fraction (Pct)	Yield Strength Increment (MPa)
1 to 5	0.077	54.5	0.015	59.0
5 to 10	0.060	61.9	0.015	33.0
10 to 18	0.105	55.0	0.021	25.0
18 to 36	0.050	23.0	0.015	13.0
Total	0.292	194.4	0.066	130.0

thinner, the cooling of hot-rolled coil is slower after coiling). The precipitation strengthening contribution of ZJ510 containing 0.18 pct carbon is greater than that of ZJ330. The precipitation strengthening contribution of ZJ330 to the yield strength is about 145 MPa.

C. *Contribution of Nanoscale Precipitates to the Yield Strength in HSLA Steel*

For HSLA steel, it is generally believed that the precipitation strengthening phase is nanoscale carbide of microalloying elements. In our research, it is found that not only the HSLC steel but also the microalloyed HSLA steels have the precipitation strengthening effects[12,13] by nanoscale iron carbon precipitates.

In considering the precipitates' contribution to yield strength, the combined contributions of precipitates with different types and sizes based on the bypass mechanism and shearing mechanism should be taken into account:

$$\sigma_{sp} = \sum_{i=1}^{n} \sigma_{sp_{1i}} + \sum_{i=1}^{n} \sigma_{sp_{2i}} \quad [4]$$

where i = nanoscale precipitate; $\sigma_{sp_{1i}}$ = precipitation strengthening contribution to the yield strength of steel based on bypass mechanism; and $\sigma_{sp_{2i}}$ = precipitation strengthening contribution to steel's yield strength based on shearing mechanism.

By calculating, the d_c of TiC is 1.5 to 6 nm and the d_c of Fe_3C is 4.7 to 10 nm. The precipitation strengthening effects of TiC precipitates with different sizes were calculated based on the bypass mechanism; for nanoscale iron carbides with less than 10-nm size, the precipitation strengthening effects of precipitates are calculated based on the shearing mechanism, and for nanoscale iron carbides with size larger than 10 nm, the precipitation strengthening effects are calculated based on the bypass mechanism. The calculated results are listed in Table XII and match the actual measured strength well (as discussed in the Section V–C).

In recent years, Zhao *et al.*[18] studied the distribution of nano cementite in 0.15 pct C, 1.50 pct Mn ferrite + pearlite steel, and found less than 100-nm-diameter ball-shaped cementite particles. The distribution of those particles is not homogeneous; the content is high in some regions.

Chakraborty *et al.*[19,20] studied the effect of bainite and martensite microstructure refinement on strengthening and toughening in HSLA bearing steel. From their study, the ultrafine grain strengthening and precipitation strengthening cannot be added directly.

Seong *et al.*[21] studied the influence of nano precipitates in BF (without boron) and BA (containing boron) low-carbon steel on mechanical properties. It was found that boron can reduce strength, improve elongation in low-carbon steel, possibly reduces solved nitrogen and carbon content, and has a negative impact on solid solution strengthening.

Three-dimensional atom probe is an appropriate tool to study nano cementite properties. Kobayashi quantitatively studied the influence of nano TiC particles on the yield strength of Fe-0.03C-0.1Ti-3Al (wt pct) steel.[22] It was found that steel strength increased with the diameter increasing of TiC precipitates when the TiC diameter was less than 3 nm, the precipitation strengthening contribution to yield strength was approximately 250 MPa.

V. COMPREHENSIVE STRENGTHENING MECHANISM

Yield strength is a stress when a large amount of dislocation starts moving at the same time; the larger

resistance to the dislocation moving means a higher yield strength of the steel. It is generally agreed that the strengthening mechanism consists of solid solution strengthening, grain refinement strengthening, precipitation strengthening, and dislocation strengthening. At the present time, there are two kinds of strengthening theories: ultrafine grain strengthening and the additivity principle of different strengthening mechanisms.

A. *Ultrafine Grain Strengthening*

In the 1950s, Hall and Petch carefully tested the fracture strengths of low-carbon steel with the carbon content of 0.036 to 0.155 pct at room temperature and liquid nitrogen temperature, and they set up the relationship between the cleavage strength and ferrite grain size for the F + P type low-carbon steel.[1] The equation is shown as follows:

$$\sigma_c = \sigma_{c0} + k_y d^{-1/2} \quad [5]$$

The effect of the grain size on the toughness of the steel was also studied by Petch. He pointed out that for the ductile-brittle transition temperature, the subsequent equation can be set up.[2]

$$T_C = a - bd^{-1/2} \quad [6]$$

where T_C is the ductile-brittle transition temperature, d is the average diameter of the grain, and a and b are constants.

From the Hall–Petch formula, the grain refinement strengthening can increase not only the strength of the steel but also its toughness.

In 1997, the national projects on the new generation steel development were conducted in Japan, Korea, and China with the support of their governments; they were named "Super steel" in Japan, "New generation steel" in China, and "High performance structure steel" in Korea. The theoretical basis and guiding thought of these projects is based on the Hall–Petch formula, regarding the ultrafine grain strengthening mechanisms of structure steels. The aim of the project is to obtain super fine grains as 1 micron meter or even submicron meter (the width of bainite or martensite lathing), thus doubling the steel strength, for the tensile strengths of low alloyed steel and alloyed steel reaching 800 and 1500 MPa, respectively. The situation is different in China; carbon steel with 400 MPa yield strength is included in the project "National Key Basic Research Program (973) of New Generation Steels." The goal of the project is to produce hot rolling coil of carbon steel with yield strength of 400 MPa and Grade III steel rebar. After 6 years of hard work from 1997 to 2003, it was found that it was impossible to obtain grain sizes of 1 micron meter in steel using the existing equipment and technology by the industrial practices in Japan. In the laboratory, the steel structure can be refined to micron meter scale *via* a special process, but grain refinement strengthening and dislocation strengthening or precipitation strengthening could not be added and the actual yield strength of steel was lower than the sum.[23]

During the same period, it was found that before and after the tempering–fast cooling for HSLC steel, the grain size did not change, as shown in Figure 11, but the yield strength of the steel improved around 100 MPa, obviously because of the nanoscaled precipitation strengthening. The contribution of precipitation

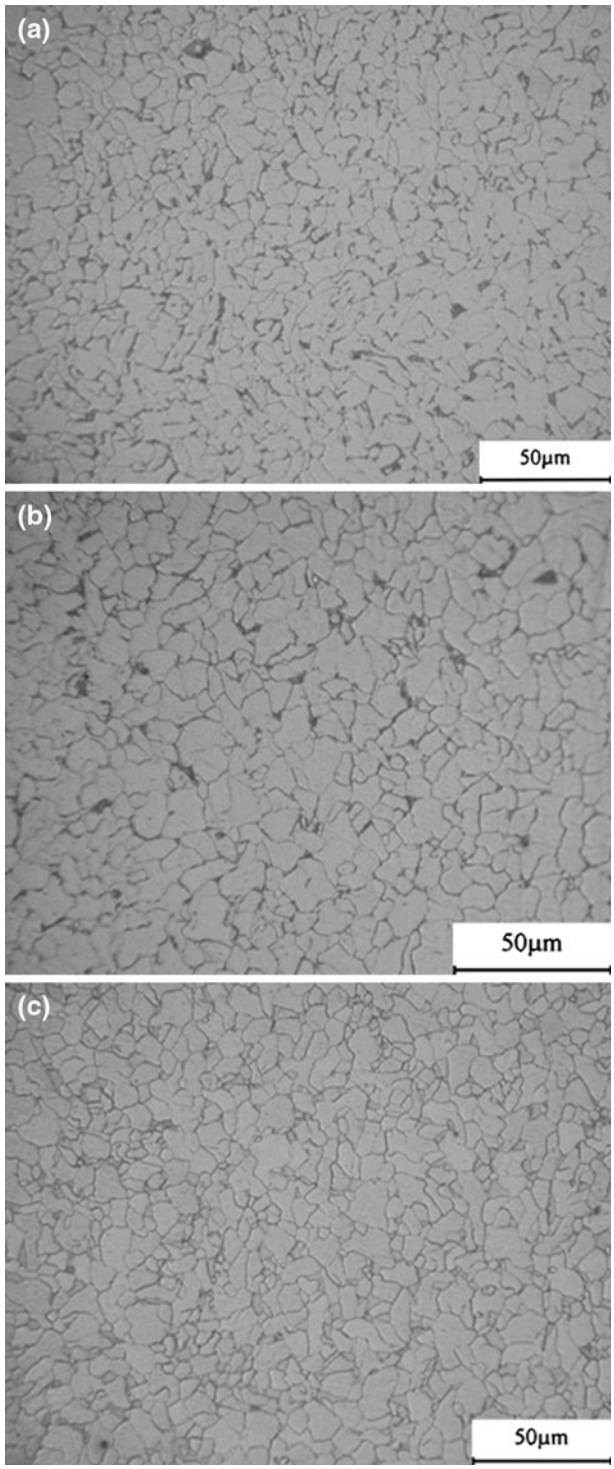

Fig. 11—Microstructure of ZJ330 steels (*a*) before and (*b*) after 873 K (600 °C) and (*c*) 973 K (700 °C) tempering–fast cooling.

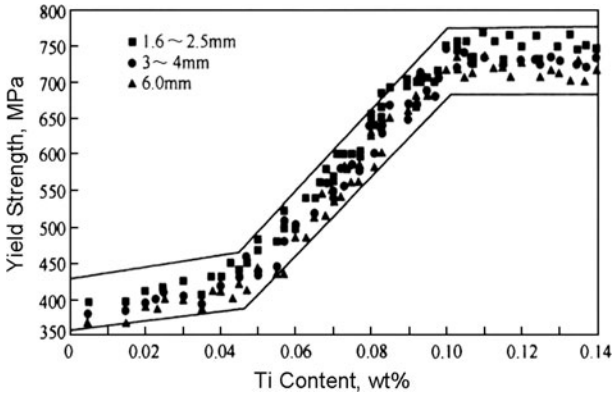

Fig. 12—Relationship between yield strength and Ti content and strip thickness of the steel.[15]

strengthening in quantity was similar to that of grain refinement strengthening.[13]

For Ti microalloyed high-strength weathering steel, the yield strength increases with the Ti content, as shown in Figure 12.

From Figure 12, we can see that the yield strength of the Ti microalloyed high-strength weathering steel increased more than 300 MPa when the Ti content in steel increased from 0.04 to 0.10 pct with the same average grain size.[15]

B. *Additivity Principle of Strengthening Mechanism*

To the steel strengthening mechanism and additivity principle, many different regression additivity formulas have been put forward. Reference 24 involves a steel strengthening additivity formula:

$$\sigma = \sigma_{\mathrm{Fe}} + \sigma_{\mathrm{C}} + \sum \sigma_{\mathrm{ss}} + K_1(L_3)^{-1} + K_2\rho_{\mathrm{d}}^{1/2} + K_3\Delta^{-1} \quad [7]$$

where σ_{Fe} is the strength of pure annealed iron; σ_{C} is the contribution of solid solution strengthening due to carbon; $\Sigma\sigma_{ss}$ is the sum of contributions to solid solution strengthening from all substitutional solutes; L_3 is the ferrite plate thickness; ρ_d is the dislocation density; Δ is the average distance between primary carbide particles; and K_1, K_2, and K_3 are material constants. In formula [7], solid solution strengthening mechanism contributes to the first three items. The last three items is grain refinement strengthening, dislocation strengthening, precipitation strengthening, respectively. The size of the alternate thin plates of ferrite formed in processes is used as the grain size of the grain refinement strengthening in References 18 and 19.

During April 2003 to March 2007, the forum on Steel Yield Strength and Microstructure was organized in Japan; the dominant structure factors on yield strength of different steel grades were investigated, and the results are reported in the Nishiyama Memorial Lecture.[23] It was reported, for low-carbon steel, that the size of the grains decreases until 1 micron meter, the yield strength of steel increases with $d^{-1/2}$ proportionally, and it is accorded with the Hall–Petch formula; the grain refinement strengthening can be calculated by formula [8]:

$$\sigma_s = 100 + 600d^{-1/2} \quad [8]$$

where σ_s is the yield strength (MPa) and d is the grain size (μm). The intercept of the Hall–Petch relation is 100 MPa, by Reference 23, in accordance with the yield strength of single-crystal iron, equivalent to solid solution strengthening. Thus, relation [8] represents the sum of solid solution strengthening and grain refinement strengthening. For different steel grades, the coefficient of $d^{-1/2}$ is different, which means that the Hall–Petch relation has a different slope and intersection and the effect of the grain size and solid solution element on yield strength is different for different steel grades. By this equation, when the grain size of low-carbon steel is 10 to 5 μm, the yield strength σ_s will be 290 to 368 MPa. However, in fact, when the grain size of HSLC ZJ330 steel is 8 to 10 μm, the yield strength σ_s reaches 410 MPa, meanwhile the elongation rate is still 29 pct.[3] For Ti microalloyed high-strength weathering steel, which contains 0.09 pct of Ti with the grain size of 2.9 to 3.8 μm,[15] the value of σ_s calculated by formula [8] is around 408 to 452 MPa, but the actual value is 700 MPa. It can be seen obviously that some other strengthening mechanism contributes to the yield strength σ_s, the difference of yield strength between the sum value of solid solution strengthening and grain refinement strengthening, and the actual value can be regarded as the result of precipitation strengthening and dislocation strengthening.

A large amount of dislocation is produced during the rolling process of steel; the interaction between the original dislocation and newborn dislocation or the resistance of the original dislocation against newborn dislocation causes dislocation strengthening or process hardening.

The contribution of dislocation strengthening to the yield strength of steel is proportional to the square root of the dislocation density, according to the Bailay Hirsch formula;[23] the sum of solid solution strengthening and dislocation strengthening can be calculated by experiential formula [9] as follows:

$$\sigma_s = 100 + 1.2 \times 10^{-5}\sqrt{\rho_{\mathrm{X-ray}}} \quad [9]$$

where σ_s is the yield strength (MPa), and $\rho_{\mathrm{X\text{-}ray}}$ is the dislocation density measured by X-ray diffraction. The solid solution strengthening is included in the intersection of formula [9]; this value corresponds to the base strength of the steel. Cold rolling can cause the iron with the maximum of dislocation density of $10^{16}/\mathrm{m}^2$, and the contribution of dislocation strengthening can reach 1200 MPa. When the density of dislocation is less than $<10^{14}/\mathrm{m}^2$ in hot-rolled steel, the contribution of dislocation will disappear.[23]

During the period of austenite recrystallization or ferrite cooling (such as coiling of hot-rolled steel plate or heat treatment), the density of dislocation will decrease. The finding that the density of dislocation of the hot-rolled coil of steel plate with thickness 1 mm is

$2.8 \times 10^{13}/m^2$ was reported.[25] Considering that the original density of dislocation is related to the pinning of the precipitated secondary phase particles, the resistance of original dislocation to the move of newborn dislocation can be ignored after calculating the precipitation strengthening of the secondary phase particles; that is, the dislocation strengthening can be ignored.

The ultrafine grain strengthening and dislocation strengthening or precipitation strengthening could not be added; the yield strength of steel is dependent on ultrafine grain strengthening adding one of both dislocation strengthening or precipitation strengthening.

It is regarded by the author of Reference 23 that ultrafine grain strengthening and dislocation strengthening or precipitation strengthening cannot be added together; this is because when the value of ultrafine grain strengthening is calculated, the width of bainite or martensite lath is adopted as the grain size; yet, accompanied with the bainite or martensite forming, a large amount of secondary phase particles and dislocation pinned by nanoscale particles precipitated in the steel, which means that ultrafine grain strengthening occurs accompanied with dislocation strengthening and precipitation strengthening. If dislocation strengthening or precipitation strengthening is added with ultrafine grain strengthening, it will be added twice. If we regard the ferrite size as grain size (approximately the grain size before martensite transform), and take into account the nanoscale precipitates in bainite or martensite, the grain refinement strengthening will agree with the Hall–Petch relationship; thus, grain refinement strengthening can be added with the precipitation strengthening.

According to the production level in the 1950s and the test method from the literature,[1] the size of the precipitates in the trial steel may be larger, so the strengthening effect could not be found; it is assumed that the carbon content and the pearlite have little effect on the strength of the steel, so only the grain size plays a decisive role in strengthening this steel.

The assumption is tenable so that the results of the theoretical calculation and the actual test are in accord and the relationship between the yield strength of several materials and the grain size of the ferrite is linear. At this time, σ_{c0} in Eq. [5] is about tens of MPa, which is the lattice friction force that expresses the influence of intragranular solute atoms on the dislocation movement.

Since the 1970s, in order to improve the strength and toughness of steel, the HSLA steel has been developed. It is found that owing to the addition of the microalloying elements such as V, Nb, and Ti, a large amount of nano microalloy carbonitride $M(C_xN_y)$ forms in the grain boundary and intragranular, which have a significant role in precipitation strengthening, and the theoretical value of the strength from the Hall–Petch formula is obviously lower than the actual value. However, the regression relationship between the yield strength and the grain size of the ferrite from the actual production data is still in accordance with the Hall–Petch formula form. Then, the formula of $\sigma_s = \sigma_{s0} + k_y d^{-1/2}$ expected by Petch can be confirmed. However, this time the formula is only an empirical formula, and under different conditions, σ_{s0} and k_y have different values. σ_{s0} expresses the contribution of other strengthening mechanisms apart from the fine grain strengthening to the strength of the steel, and k_y expresses the influencing degree of the grain size on the strength of the steel under certain conditions, which have different physical meanings than the original formula of Eq. [1]. Therefore, we should carefully consider the application scope of the formula.

The strength of either low-carbon steel or microalloyed steel caused by solid solution strengthening is normally dozens of MPa. The higher contents of alloy elements in steel indicate the higher contribution of solid solution strengthening.

C. *Quantitative Calculation of Yield Strength by Comprehensive Strengthening Mechanism for Steel*

The contribution of nanoscale TiC with size less than 36 nm to the yield strength of Ti alloyed steel was calculated by the present author according to formula [1]. The result is shown in Figure 13.

The result shows that the contribution of TiC precipitate to the yield strength increment of the Ti microalloyed high-strength weathering steel with 0.09 pct Ti is 130 MPa, 200 MPa lower than the actual yield strength. Exploring the reason, it was thought that the contribution of nano precipitate Fe_3C was ignored in Reference 15.

The effect of the nanoscale Fe_3C precipitate on the yield strength of steel is discussed in this article; it is found that, except nanoscale MC, there exists nanoscale M_3C; the contribution of M_3C precipitate to the Ti microalloyed high-strength weathering steel with 0.09 pct Ti content reaches 194 MPa (refer to Table XII).

The comprehensive strengthening mechanism for steel is "the yield strength equals all the contribution coming from all kinds of strengthening mechanisms," which is a "modified additivity principle of the steel strengthening mechanism." For low-carbon steel, it is regarded that the yield strength of steel equals the sum of solid solution strengthening, grain refinement strengthening, and precipitation strengthening.

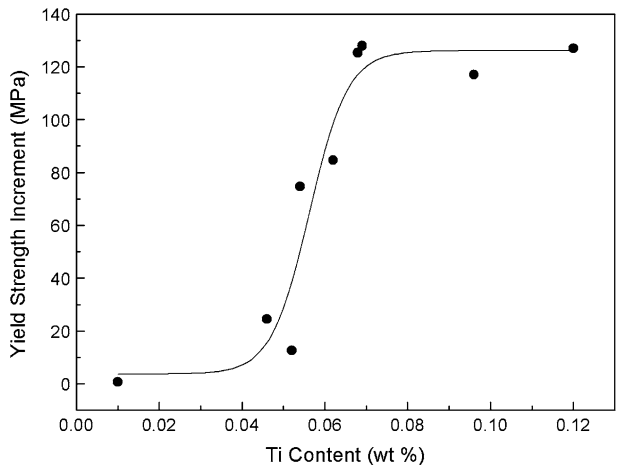

Fig. 13—Contribution of nanoscaled TiC with size less than 36 nm to the strength of Ti microalloyed steel.

That is,

$$\sigma_s = 100 + 600 \times d^{-1/2} + \sum_{i=1}^{n} \frac{5.9\sqrt{f}}{d_{1i}} \ln\left(\frac{d_{1i}}{2.4 \times 10^{-4}}\right) + \sum_{i=1}^{n} \frac{2.2}{\sqrt{2AG}} \times \frac{\gamma^{3/2}}{b^2} \times d_{2i}^{1/2} f^{1/2};\ d_{1i} \geq d_c \geq d_{2i} \quad i = 1, 2, \ldots, n \quad [10]$$

In formula [10],

σ_s = yield strength, MPa;
i = nanoscale precipitate;
d_{1i} = the diameter of nanoscale precipitate by which the precipitation strengthening should be calculated by the bypassing mechanism, μm; and
d_{2i} = the diameter of nanoscale precipitate by which the precipitation strengthening should be calculated by the incision mechanism, μm.

The values of σ_s calculated by formula [10] agree with the actual measured values, as shown in Table XIII.

VI. APPLICATIONS OF PROPOSED STRENGTHING MECHANISM

A. *Development of Low-Cost High-Strength Steel*

1. *HSLC steel*

According to the Hall–Petch equation, for Q195 and Q235 steel, it is impossible to improve the yield strength from 200 to 400 MPa by the traditional process. On the basis of that, there existed a large amount of nanoscale Fe_3C precipitates in hot-rolled coil produced by CSP line. Guangzhou Zhujiang Steel Co., Ltd., in cooperation with the University of Science and Technology Beijing, developed HSLC steel; it is a one-of-a-kind low-carbon Mn series steel without microalloying elements such as V, Nb, and Ti, and its mechanical properties are similar to the HSLA steel with similar content of carbon and manganese, as shown in Table XIV.

HSLC steel has the property of isotropy, the ratio of transverse and longitudinal yield strength, and tensile strength, and the ratio of elongation is around 0.96 to 1.10.[11]

HSLC steel has the performances of high strength, plasticity, and toughness. The mechanical performances and low-temperature impact toughness of automobile plate ZJ510L are shown in Tables XV and XVI.

2. *Container plate steel and Ti microalloyed high-strength weathering steel*

Zhujiang Steel, in cooperation with the University of Science and Technology Beijing, developed SPA-H container steel with C ≤ 0.07 pct, Mn 0.25 to 0.5 pct, Si 0.25 to 0.50 pct, P 0.07 to 0.12 pct, S ≤ 0.01 pct, N < 0.005 pct, and Al < 0.04 pct. By controlling low C, low N in composition, controlling rolling, and cooling in process, the total amount of alloy is less than 1 pct, with σ_s higher than 400 MPa. The annual output of container steel of Zhujiang Steel is more than 25 pct of the total amount output of the world.

Table XIII. Comparison of Calculated Yield Strength Values with Those of Actual Measured

Steel Grade	Grain Size d (μm)	Calculated Yield Strength Values, MPa: Contribution of Solid Solution Strengthening and Grain Refinement Strengthening	Calculated Yield Strength Values, MPa: Contribution of Precipitation Strengthening	Calculated Yield Strength Values, MPa: σ_s	Actual Measured σ_s (MPa)
ZJ330	8 to 10	189 to 212	145	334 to 357	330 to 390
ZJ510	5	268	202	470	408 to 492
Ti microalloyed high-strength steel with thickness of 3 mm	2.9 to 3.8	307 to 352	324	631 to 676	630 to 680

Table XIV. Comparison of Chemical Composition and Room-Temperature Strength in 400 MPa Steel Grades

Steel Grade	Thickness (mm)	C (Mass Pct)	Mn (Mass Pct)	Si (Mass Pct)	P (Mass Pct)	S (Mass Pct)	Al (Mass Pct)	N (Mass Pct)	σ_s (MPa)	σ_b (MPa)	δ (Pct)
Q195	≤16	0.06 to 0.12	0.25 to 0.50	≤0.30	≤0.045	≤0.050	≥0.015		195	315 to 430	>33.0
Zhujiang steel	2.0 to 6.0	0.05	0.3	0.06	≤0.020	0.0049	0.02 to 0.04	<0.0050	387	433	33.0
Q235	≤16	0.14 to 0.22	0.30 to 0.65	≤0.30	≤0.045	≤0.050	≥0.015		235	375 to 500	>26.0
Zhujiang steel	6	0.06	0.61	0.17	0.017	0.006	0.015	<0.0050	439	494	31.5
16Mn	≤16	≤0.20	1.0 to 1.6	≤0.30	≤0.045	≤0.055	≥0.015		345	470 to 630	21.0
ZJ510	6	0.17	1.21	0.28	0.023	0.004	0.024	<0.0050	492	597	27.8
	6	0.16	1.22	0.3		0.003	0.037	<0.0050	408	566	34.0
Overseas HSLA	6.3	0.055	1.1				Nb: 0.045	0.009	456 402	547 486	32.2 32.7

Table XV. Average Mechanical Performance of ZJ510L

Thickness (mm)	Transverse				Longitudinal			
	σ_s (MPa)	σ_b (MPa)	δ (Pct)	Ratio of Yield Strength to Tensile Strength	σ_s (MPa)	σ_b (MPa)	δ (Pct)	Ratio of Yield Strength to Tensile Strength
4.5	445	580	34	0.77	440	575	31	0.77
6	455	602	26	0.76	457	605	27	0.76
8	437	585	26	0.75	427	572	28	0.75
10	415	565	26	0.73	435	580	26	0.75

Table XVI. Charpy Impact Energy Akv of ZJ510L and ZJ550L, Joule

Steel Grade	Thickness (mm)	Room Temperature	273 K (0 °C)	253 K (–20 °C)	233 K (–40 °C)	213 K (–60 °C)	193 K (–80 °C)	173 K (–100 °C)
Q345	≤16	≥34	≥34	≥34	≥27	—	—	—
ZJ510L	6	52	48	44	43	33.5	25.5	6
ZJ550L	5	52	51	50	49	42.5	28.5	27
ZJ550L	6.5	63	57	56	53	33.0	17.5	7.5
ZJ550L	8	60	57	55	45	35.0	23.5	9.5

Table XVII. Effect of Reducing Weight of New Generation Lightweight Container

Container type	20'DV	40'HC
New generation container weight (kg)	1900	3350
Common container weight (kg)	2220	3840
Weight reduction (kg)	320	490
Ratio of weight reduction (pct)	15.2	14.5

In order to develop container steel with σ_s higher than 450 MPa, Ti microalloyed high-strength weathering steel was developed under the laboratory scale and industrial production, precipitation strengthening was considered to obtain high strength. The relationship of the yield strength of the steel and Ti content is shown in Figure 12 and referred to Reference 15.

The series grades of Ti microalloyed high-strength weathering steel were developed at Zhujiang Steel;[26] steel with different Ti contents has unique yield strength. The weight of a container that is made of Ti microalloyed 550 MPa high-strength weathering steel is 15 pct lighter than that made of Ti microalloyed 400 MPa steel (Table XVII).

3. *Other steel grades under development*

Some steel grades are under development, as shown in Table XVIII, by the union of the University of Science and Technology Beijing, Wuhan University of Science and Technology, and Valin Lianyuan Steel.[27,28]

B. *Steel Softening*

Steel softening was studied by the author of Reference 29; the tensile strength of ZJ33 decreased from 350 to 250 MPa by tempering and then slow cooling nearly above the temperature of A1. The results are shown in Table XIX.

C. *UHU Process on the Basis of Nanoscale Fe_3C Precipitation Controlling*

The academician, Mr. Guodong Wang, invented a process of ultrafast cooling (UFC), according to the viewpoint of controlling the precipitate in the steel during the production process; it was considered that the process of UHU, in other words, the process of UFC-holding-UFC has an important meaning to the production of wide and heavy plate. Similar to the heat history of CSP hot-rolled strip, continuous cooling can make the thick plate have a more uniform volume fraction of nanoscale precipitates in the center and the edge of the whole plate, which means the plate has a uniform high strength; thus, high-strength steel can be produced with lower cost.

D. *Technical Analysis of Advanced High-Strength Steel with σ_b Being 1500 MPa*

One of the research goals of advanced high-strength steel is to produce the structure steel with σ_b being 1500 MPa in both China and Korea. According to the theory of the comprehensive strengthening mechanism of steel and the control of nanoscale precipitates in the steel, it is considered by the author that in the production of the structure steel with σ_b being 1500 MPa, technical measures should be taken as follows.

1. *Enhancing the contribution of solid solution strengthening*

According to Orowan's mechanism, when the size of nanoscale precipitates is larger than 40 nm, their strengthening contribution will be small. Fe_3C precipitates less than 40 nm and carbides of other elements will consume a few carbon under fast cooling conditions, so increasing carbon content in the steel will increase the

Table XVIII. Other Steel Grades Under Development

Content (Mass Pct)	C	Mn	Si	S	P	N	Al	Ti	Remarks
Steel rebars	≤0.06	<2.0	<1.0	≤0.004	≤0.020	<0.005	0.01 to 0.03	< 0.1	high-strength steel bars with low cost
Pipeline steel	0.046	1.45	0.23	0.003	0.007		0.03	0.09	series above X70 with low-cost
Engineering machinery steel	≤0.06	≤2.0	≤0.5	≤0.004	≤0.018		0.025 to 0.05	≤0.1	steel strength over 700 MPa with low cost

Table XIX. Effect of the Tempering-Slow Cooling near Temperature of A1 on the Mechanical Properties of ZJ330 Steel[29]

Process of Heat Treatment	Temperature [K (°C)]		σ_s	σ_b	σ_s/σ_b	δ (Pct)
Heating and holding at X K for 20 min, furnace Cooling to room temperature	X	873 (600)	322	397	0.81	43
		973 (700)	310	370	0.83	46
		1033 (760)	265	335	0.79	51
		1073 (800)	225	310	0.72	50
Heating and holding at 1073 K (800 °C) for 20 min, furnace cooling to Y K, and then further water cooling to room temperature	Y	973 (700)	305	400	0.76	34
		873 (600)	250	360	0.69	35
		773 (500)	245	345	0.71	36
		673 (400)	245	340	0.72	40

content of carbon in solid solution. Carbon as solute makes a remarkable contribution to solid solution strengthening. Furthermore, increasing the contents of other alloying elements will enhance the contribution of solid solution strengthening.

2. *Enhancing the contribution of precipitation strengthening*

The nanoscale carbides of V, Nb, Ti, and Mo will enhance the contribution of precipitation strengthening; meanwhile, the contribution of nanoscale Fe_3C precipitate should not be neglected. The effect of V, Nb, Ti, and Mo on nanoscale Fe_3C should be studied.

3. *Increasing tempering temperature and cooling speed*

The treatment of quenching and tempering is normally adopted in the production of high-strength structure steel with σ_b being 1500 MPa. According to the result of tempering–fast cooling experiments, the speed of carbon dispersion is quick at the temperature of 873 K (600°C); the adoption of the process of tempering temperature around 873 K (600°C) and water cooling after tempering is recommended.

4. *Contribution of grain refinement strengthening*

Normally, there exists bainite, martensite in high-strength structure steel with σ_b being 1500 MPa; the grain size of austenite should be refined before transforming by control rolling and control cooling, in order to enhance fine grain strengthening. The refined austenite grain size should be taken as the parameter of the formula of Hall–Petch.

5. *Improving the cleanness of the steel*

According to the comprehensive strengthening mechanism of steel, not only the cooling process after rolling should be controlled but also the metallurgical quality of steel should be controlled; improving the cleanness of the steel is the basis of enhancing the contribution of nanoscale precipitates.

VII. CONCLUSIONS

1. The measurement of volume fraction and size distribution of nanoscale cementite precipitates in steel were carried out by using chemical phase analysis and XSAS. There existed the nanoscale cementite precipitates with size less than 18 nm in HSLC steel, and that with size less than 36 nm in Ti microalloyed high-strength weathering steel. The volume fraction of Fe_3C is 4.4 times as that of Ti (C, N) in the same size range in Ti microalloyed high-strength weathering steel.
2. The comprehensive strengthening mechanism of steel is ''the yield strength equals the total amount of all kinds of strengthening mechanism contribution,'' which is 'the modifying additivity principle of strengthening mechanism.'' For low-carbon steel, the calculation formula is proposed. The calculated yield strength corresponded to the actual measured result.
3. The interaction among precipitation strengthening and dislocation strengthening, phase transformation, and phase structure and the effect mechanism of microalloying elements V, Nb, Ti, and Mo, and the type and precipitation kinetics of nanosized precipitates are waiting for further study.

ACKNOWLEDGMENTS

We are thankful for the financial support of the National Natural Science Foundation of China (Grant

No. 50334010) and the National Key Basic Research Program (973) of New Generation Steels (Grant No. G1998061500). The authors also thank the senior member of the Chinese Academy of Science, Jun Ke (T. Ko) for his supervision, encouragement, and support. Thanks to Professor Delu Liu, Professor Yonglin Kang, and Dr. Zhongbing Wang for their help in the research. Thanks to Professor Yueguang Yu for supporting the research work. Thanks are also extended to Drs. Huajie Wu, Jian Yu, Jianfeng Wang, and Xian Fan for their hard work in this research.

REFERENCES

1. N.J. Petch: *J. Iron Steel Inst., London*, 1953, vol. 174, pp. 25–28.
2. N.J. Petch: *Philos. Mag.*, 1958, vol. 3, pp. 1089–97.
3. T. Gladman, D. Dulier, and I.D. Mclvor: *Structure-Property Relationships in High Strength Microalloyed Steels*, Microalloying 75, ASM, New York, NY, Union Carbide Corporation, Niagara Falls, NY, 1977, pp. 32–54.
4. Q. Yong, M. Ma, and B. Wu: *Microalloyed Steel, Physical and Mechanical Metallurgy*, 1st ed., Mechanical Industry Press, Beijing, 1989, pp. 80–81.
5. T. Semuma: *ISIJ Int.*, 2002, vol. 42, pp. 1–12.
6. Q. Yong: *The Secondary Phase in Metal Material*, Metallurgical Industry Press, Beijing, 2006, pp. 15–17.
7. D. Liu, J. Fu, Y. Kang, X. Huo, Y. Wang, N. Chen, Z. Wang, and L. Li: *J. Mater. Sci. Technol.*, 2002, vol. 18, pp. 7–9.
8. D. Liu, X. Huo, Y. Wang, and X. Sun: *J. Univ. Sci. Technol. Beijing*, 2003, vol. 10, pp. 1–6.
9. Y. Kang, H. Yu, J. Fu, K. Wang, and Z, Wang: *Mater. Sci. Eng*, 2003, vol. A351, pp. 265–71.
10. J. Fu, Y. Liu, and H. Wu: *Sci. China, Ser. E: Technol. Sci.*, 2008, vol. 51, pp. 989–98.
11. J. Fu: *Chin. J. Nonferrous Met*, 2004, vol. 14 (s1), pp. 82–90.
12. J. Fu, Y. Kang, D. Liu, D. Zhou, Z. Wang, and G. Chen: *J. Univ. Sci. Technol. Beijing*, 2003, vol. 25, pp. 328–31.
13. J. Fu, H. Wu, and Y. Liu: *Sci. China, Ser. E: Technol. Sci.*, 2007, vol. 50, pp. 166–76.
14. Z. Wang, H. Wu, and J. Fu: *Proc. Int. Symp. on Thin Slab Casting and Rolling (TSCR)*, Guangzhou, China, 2006, pp. 56–62.
15. X. Mao: *Microalloyed Technology on Thin Slab Casting and Rolling*, Metallurgical Industry Press, Beijing, 2008, pp. 88–90.
16. K. Fang, G. Wang, X. Wang, L. Huang, and G. Deng: *Science and Processing of Cast Iron VIII, Proc. 8th Int. Symp. on Science and Processing of Cast Iron*, Beijing, Oct. 16–19, 2006, pp. 181–87.
17. K. Fang, L. Zheng, K. Fang, and L. Fuang: *China Particuol.*, 2003, vol. 1, pp. 88–90.
18. M.-C. Zhao, T. Hanamura, H. Qiu, K. Nagai, and K. Yang: *Scripta Mater.*, 2006, vol. 54, pp. 1193–97.
19. J. Chakraborty, K. Bhattacharjee, and I. Manna: *Scripta Mater.*, 2009, vol. 61, pp. 604–07.
20. J. Chakraborty, P.P. Chattopadhyay, D. Bhattacharjee, and I. Manna: *Metall. Mater. Trans. A*, 2010, vol. 41A, pp. 2871–79.
21. B.S. Seong, Y.R. Cho, E.J. Shin, S.I. Kim, S.-H. Choi, H.R. Kim, and Y.J. Kim: *J. Appl. Cryst.*, 2008, vol. 41, pp. 906–12.
22. Y. Kobayashi, J. Takahashi, and K. Kawakami: *CAMP-ISIJ*, 2010, vol. 23, p. 403.
23. S. Takaki: *Ferrum*, 2008, vol. 13, pp. 304–09.
24. C.H. Young and H.K.D.H. Bhadeshia: *Mater. Sci. Technol.*, 1994, vol. 10, pp. 209–14.
25. Y. Kang, J. Fu, D. Liu, and H. Yu: *The Structure Properties Control of the Steel Produced by CSP Line*, Metallurgical Industry Press, Beijing, 2006, pp. 375–76.
26. X. Mao, X. Huo, X. Sun, and Q. Chen: *Proc. Int. Symp. on Thin Slab Casting and Rolling (TSCR)*, Nanjing, China, 2009, pp. 306–13.
27. G. Li, J. Wang, D. Wen, A. Xiao, and J. Fu: *Proc. Int. Symp. on Thin Slab Casting and Rolling (TSCR)*, Nanjing, China, 2009, pp. 400–05.
28. L. Chen, Y. Kang, and D. Wen: *Proc. Int. Symp. on Thin Slab Casting and Rolling (TSCR)*, Nanjing, China, 2009, pp. 371–76.
29. J. Fu, H. Wu, and C. Liu: *Chin. Eng. Sci.*, 2008, vol. 10, pp. 65–71.